CHEMISTRY OF MATERIALS

ARTICLE

pubs.acs.org/cm

Substrate Reactivity Effects in the Atomic Layer Deposition of Aluminum Oxide from Trimethylaluminum on Ruthenium

Massimo Tallarida,*[,†] Kaupo Kukli,[‡,§] Marcel Michling,[†] Mikko Ritala,[‡] Markku Leskelä,[‡] and Dieter Schmeisser[†]

[†]Department of Applied Physics-Sensors, Brandenburg University of Technology, Konrad Wachsmann Allee, 17, D-03046 Cottbus, Germany

[‡]Department of Chemistry, University of Helsinki, P.O. Box 55, FIN-00014 Helsinki, Finland

[§]Institute of Experimental Physics and Technology, University of Tartu, Tähe 4, EE-51010 Tartu, Estonia

ABSTRACT: A detailed study of the atomic layer deposition of Al_2O_3 on Ru film surfaces by means of in situ photoelectron spectroscopy has been carried out. We discuss how the atomic layer deposition reaction between trimethylaluminum (TMA) and H_2O is affected by the Ru substrate. We found that RuO_2, when present on the substrate surface, participates in the reaction with TMA and the substrate reduces to Ru. The reduction of oxygen-containing substrates to Ru is solely due to the direct reaction of the Al precursor with the substrate through adsorption on active sites. The final Al_2O_3/Ru structures have an interface depleted from oxygen and show different band offsets depending on the initial chemistry.

KEYWORDS: atomic layer deposition, Al_2O_3, Ru, RuO_2, in-situ XPS, synchrotron radiation, photoelectron spectroscopy, reactivity, surfaces, interfaces, thin films

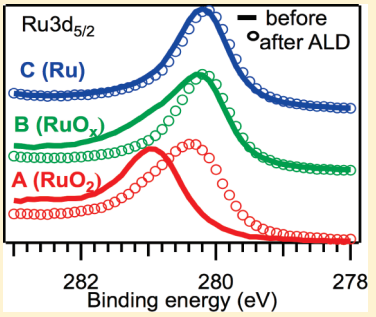

INTRODUCTION

When ALD is compared to chemical vapor deposition, the main difference is the sequential exposure of the substrate to the precursors.[1] This leads to the reaction of each single precursor species with the surface. Hence, the presence of the substrate surface is a very important component in the development of the chemical reactions leading to film growth. For example, the substrate may offer active adsorption sites that facilitate reactions otherwise unfavorable[2] upon lowering their activation barrier.

Recently, some papers have stressed the importance of substrates in ALD. For instance, Kim et al. and Choi et al.[3,4] observed ALD growth of rutile TiO_2 films at exceptionally low temperatures on O_3 pretreated Ru. They addressed that feature to the formation of a RuO_2 rutile structure through O_3 pretreatment (Ru surface exposed to O_3 at 250 °C),[3] which directed the growth of TiO_2 to the structure with a small lattice mismatch to RuO_2. This follows a typical concept of epitaxial growth mechanisms.[5] Baker et al.[6] used a similar physical interpretation related to the use of wetting layers in growth dynamics to explain the different incubation properties of Pt ALD on either Al_2O_3 or W substrates. They observed that to reduce the incubation time of Pt growth on Al_2O_3 the presence of a W adhesion film was necessary. They explained this by considering the physical properties of W that has a larger surface energy than Pt, allowing the growth of smooth and uniform Pt films.[6]

Kukli et al.[7] reported the ALD of Ru by oxidative decomposition of 1-ethyl-1′-methyl-ruthenocene (EMR) with O_2, finding that the nucleation behavior and the sheet resistance of Ru films were strongly influenced by the substrate material and, more interestingly, also by the substrate layer preparation parameters. The substrates used in that study were oxide layers (Al_2O_3, HfO_2, TiO_2, and ZrO_2) grown by ALD. For substrate layers grown at higher temperatures, the Ru ALD nucleated better, and the resistivity of Ru was lower than on substrates grown at lower temperatures. The authors correlated that behavior partially to the ionicity of the substrate material and partially to the crystallization of the substrate oxide at higher temperature, probably delivering a large number of defective grain boundaries. However, those considerations tacitly imply that the mechanisms leading to the growth of Ru were of the Mars-van Krevelen type.[8,9] Mars-van Krevelen reactions are often used for hydrocarbon oxidation, where the catalyst and the hydrocarbon interact in the reactor, the catalyst being reduced to a certain extent, while the hydrocarbon is oxidized by the oxygen from the catalyst lattice.

These three examples show that the chemical and physical properties of the substrate used for ALD may induce differences in the evolution of the growing film. However, there is a fundamental difference between the first two examples and the last one. The first two examples show how equilibrium properties (crystal structure and surface/interface energy) of the final system (substrate + thin film) lead to different features. The equilibrium properties of a system are independent of the growth method used and are characteristic of the system. The last example, instead, indicates that the properties of the substrate influence the ALD reactions during thin film formation. In this case, according to the particular ALD precursors and parameters used for the material grown, the substrate surface may lead to different properties of the material (e.g., sheet resistance). In this

Received: January 27, 2011
Revised: May 18, 2011
Published: June 13, 2011

ACS Publications © 2011 American Chemical Society

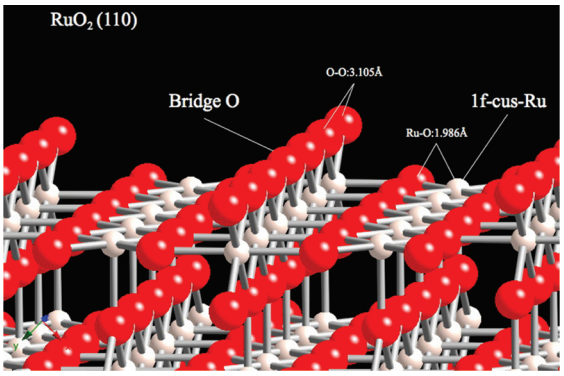

Figure 1. Ball and stick model of the rutile RuO_2(110) surface. The bridge oxygen and coordinatively unsaturated Ru sites (1f-cus-Ru) are indicated.

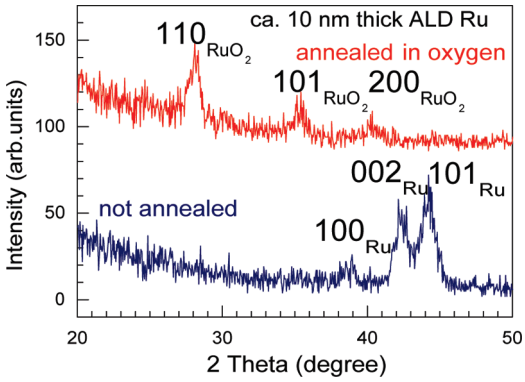

Figure 2. Grazing incidence X-ray diffraction (GIXRD) pattern recorded using 1° incidence angle of a not annealed Ru sample (lower pattern) and of a sample annealed in oxygen (upper pattern). The influence of annealing in ambient oxygen is observed by the changes in the diffraction pattern.

article, we want to address the importance of the substrate in ALD pointing out how the composition of the substrate allows different ALD routes and influences the final material properties.

As observed in many theoretical investigations,[10−14] the ALD reactions go through many intermediate steps that have a local endothermic or exothermic character. The activation barriers for the intermediate steps might be of decisive importance in ALD growth. For example, Jeloaica et al.[12] showed that the chemisorption of TMA on a Si−H substrate goes through four steps. They found that the most important step (the third), connected to the reaction of TMA with the substrate and the removal of one $-CH_3$ group, had a larger barrier (about 1 eV) than desorption (about 0.5 eV).[12] From this energetic property, the authors deduced that the desorption was more probable than the removal of the $-CH_3$ group, influencing the sticking coefficient as desorption of TMA leads to fewer ALD reactions. Indirectly, this behavior influences the growth rate per cycle (GPC) as it is governed by the equilibrium between ligand-exchange reactions and the desorption of the unreacted precursor. From this example, one may see that a different substrate would possibly decrease the barrier energy of that particular step, changing the equilibrium property of the entire reaction and eventually increasing the GPC. The way, the substrate may participate in ALD by shifting the equilibrium of one or the other reaction is therefore very interesting when studying the properties of ALD films. We want also to remark that these properties are especially important for ALD because they concern the precursor−substrate reactions alone.

Ruthenium and RuO_2 are technologically important materials as high work-function electrodes in metal−insulator−metal (MIM) capacitors[15] and as metal gates in p-type metal−oxide−semiconductor (PMOS) structures.[16] Their work function is about 5 eV and may reach 6 eV depending on the surface reconstruction and/or the presence of adsorbates.[17,18] Ru is also used as a barrier and seed layer in damascene Cu plating for interconnect formation.[19] Because of its importance in microelectronics, Ru has been subject of various investigations regarding the growth of conformal thin films by ALD[7,20−22] and the oxidation/reduction behavior of the effective work function in high-k/Ru systems.[18,23] Ru was also extensively investigated as a catalyst in many reactions, but the most interesting catalytic property of Ru resides in the strong activity of RuO_2(110) surface in redox reactions of the Mars−van Krevelen type.[8,24] The catalytic activity of RuO_2 is probably due to its rutile crystal structure similar to that of TiO_2, having bridged oxygen sites and coordinatively unsaturated Ru sites (1f-cus-Ru in Figure 1) that are very reactive toward adsorption[24] due to the dangling bond associated with them. Nonoxidized metallic Ru is stable in the hexagonal structure.[24−26]

Trimethylaluminum (TMA) is one of the most studied and used ALD precursors. It is very reactive and gives overall good quality Al_2O_3 films. The reactions of TMA with various substrates were extensively studied both experimentally, with in situ FTIR[27,28] and mass spectrometry,[29,30] and theoretically.[10−14,31] One of the best ALD precursor/substrate systems to study is given by TMA/Ru-RuO_2 because of the high activity of the Ru-RuO_2 system and the high reactivity of TMA. Indeed, Won et al.[32] studied the ALD of TiO_2 and Al_2O_3 on Ru and RuO_2 finding a high growth rate per cycle and attributed the behavior to the oxygen diffusion from the substrate toward the ALD film. Finally, in a very recent publication Lee et al.[33] observed for the TiO_2 ALD on Ru and RuO_2 a substrate-enhanced growth mode. However, they found a different behavior for different oxygen sources (H_2O and O_3). Moreover, they observed that RuO_2 was reduced completely to metallic Ru during TiO_2 film growth.

In this study, we use the high surface sensitivity of synchrotron radiation−photoemission spectroscopy (SR-PES)[34] to show that by using TMA as the Al_2O_3 precursor the properties of the film and of the whole system may be varied by modifying the Ru-based substrate. Hence, we report observations on the differences in band alignment and growth mode of Al_2O_3 by ALD on differently prepared Ru films due to different ALD reaction routes. The phenomena observed are of course important only at the beginning of growth and in very thin films. Our findings show that the properties of the substrate surface should be considered in this case. We address the role of the substrate in ALD with TMA by pointing out the reactive properties of the substrate. For this purpose we used an UHV-compatible ALD reactor developed at the Brandenburgische Technische Universität (BTU), Cottbus, for performing in situ measurements.[35]

EXPERIMENTAL DETAILS

Thin Ru films were deposited by means of ALD on ZrO_2 substrates using (ethylcyclopentadienyl)(pyrrolyl)ruthenium (ECPR) (Praxair, Inc.). Depositions were carried out in a commercial flow-type hot-wall ALD reactor F120 (ASM Microchemistry)[1] at 325 °C. Ru films were formed via oxidative decomposition of the adsorbed metal precursor layers by air pulses. The films were deposited by applying 130 growth

dx.doi.org/10.1021/cm200276z |Chem. Mater. 2011, 23, 3159–3168

Table 1. Preparation Parameters of Samples A−D[a]

sample	temperature (°C)	gas	gas pressure (mbar)	time (s)	gas dose (L)	denotation
A	400	O_2	3×10^{-4}	300	5.6×10^4	RuO_2
B	200	O_2	2×10^{-4}	300	3.7×10^4	RuO_x
C	300	H_2	9×10^{-5}	300	1.7×10^4	Ru
D	400	O_2	3×10^{-4}	300	5.6×10^4	RuO_2^*

[a] Differently from the first three samples, sample D was not sputter-cleaned before oxidation.

cycles with cycle times of 4−2−12−4 s for the sequence ECPR pulse−purge−air pulse−purge. The ruthenium films clearly demonstrated hexagonal structure as proven by grazing incidence X-ray diffraction (GIXRD) measurements. The structure was identified as hexagonal Ru (PDF Card 06-0663) metal (Figure 2) for the as-deposited films, while the films annealed in O_2 atmosphere (see Table 1) showed the rutile RuO_2 structure (PDF Cards 40-1290 and 43-1027). Formation of RuO_2 was not recognized by XRD in the films not subjected to annealing. Approximately 5−7 nm thick films were grown, possessing sheet resistance of 60 Ω/□ and resistivity in the range of 30−40 μΩcm.[36] From the same Ru substrate, we prepared samples with varying oxygen content. First we sputter-cleaned the samples with He^+ (10^{-6} mbar, 4.5 keV, 45′) and then annealed the samples under different conditions.

In Table 1 are listed the preparation procedures for all samples. Samples A−D will be hereafter alternatively denoted as RuO_2, RuO_x, Ru, and RuO_2^*, respectively. The chemical properties of the four samples after the substrate preparations and after the last ALD cycle were checked by X-ray photoelectron spectroscopy (XPS) using a nonmonochromatic Mg−Kα source (1253.5 eV) in normal emission geometry. SR-PES was performed at BESSY-II in Berlin, Germany. Substrates A−C were characterized by measuring the Al2p and Ru4p peaks, and the valence band at 121 eV on the TGM7 beamline, allowing a photon range of 10−125 eV. Measurements were done after their preparations and after 5 complete ALD cycles to follow Al_2O_3 growth. The work function (WF) was determined by measuring the secondary electrons onset with 20 eV photons and applying a bias to the sample of 10 eV. Sample RuO_2^* was measured on the U49-2/PGM2 beamline,[37] allowing photons with energy between 85 eV and 1800 eV. In this case, SR was used to measure the Ru3d and O1s peaks with variable photon energy for changing the surface sensitivity of photoemission. All photoemission spectra were measured using a PHOIBOS-150 electron analyzer by SPECS Surface Nano Analysis GmbH equipped with a 2D-CCD detector system and a multichannel-plate (MCP). The synchrotron radiation spectra were all measured using a 45° emission angle. The lens modus of the electron spectrometer was set to have a large (8°) angular integration.

Al_2O_3 films were deposited by ALD using TMA and H_2O as precursors. N_2 was used as purging gas. In all experiments reported here, the substrate temperature was kept at 280 °C. The ALD of Al_2O_3 was performed in an UHV-compatible ALD reactor built at the BTU-Cottbus, connected to the experimental station through a valve.[35] The samples were prepared in the ALD reactor and then transferred into the measurement chamber without breaking the vacuum. The samples were heated to the required temperature within a few seconds. After performing ALD at 10^{-3} mbar, the pressure recovered to 5×10^{-8} mbar within a few minutes, and the sample was transferred into the measurement chamber. The TMA pulse was 0.5 s, and the H_2O pulse was 1 s. The N_2 pulse (0.3 s) was performed two times after each precursor pulse to definitely purge the chamber.

RESULTS AND DISCUSSION

XPS Characterization before and after ALD. The XPS characterization of RuO_2 and RuO_x samples before ALD of Al_2O_3 revealed the presence of Ru−O bonds, as determined by the binding energy (BE) position (280.5−280.8 eV) and the line-shape of Ru3d (Figure 3) and of O1s peaks (Figure 4). The Ru sample, instead, showed the typical Ru3d peak of elemental Ru (BE = 280.1 eV). It is worth noting that the formation of RuO_2 in sample A (and D) is assured by the presence of the typical satellite structure in the Ru3d core level[25] at about 282.5 eV, while it is not clearly observable in any other sample, meaning that only those samples have an extended RuO_2 composition, while sample B has only a thin RuO_x film.[38−40]

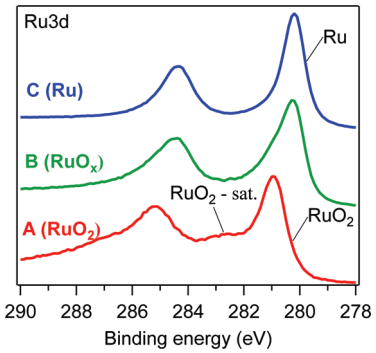

Figure 3. Ru3d spectra of samples A−C. The position of Ru^{0+} and Ru^{4+} are indicated. Sample A has a marked RuO_2 satellite at 282.5 eV.

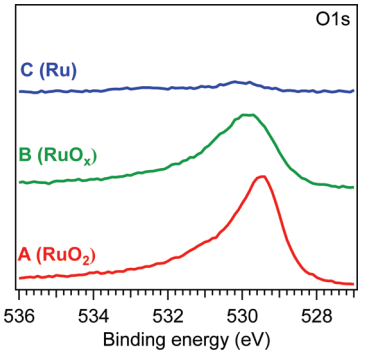

Figure 4. O1s spectra of samples A−C. The different photoemission intensities indicate the different amounts of oxygen included in the substrates.

This consideration allows us the denotation of sample A (D) as RuO_2 (RuO_2^*) and sample B as RuO_x. The O1s spectra confirm the formation of RuO_2 on sample A through the peak at 529.5 eV ("bulk" RuO_2 component)[39] and the small tail at 528.7 eV (bridge O on the RuO_2(110) surface).[39] The presence of the low energy tail reveals also the extended nature of RuO_2 and its relatively good quality with only a limited number of defects. The RuO_x sample has a weak component at 529.5 eV, but the main peak is centered at 530 eV. This further confirms that sample B has mainly a "surface oxide" with some RuO_2

dx.doi.org/10.1021/cm200276z |Chem. Mater. 2011, 23, 3159–3168

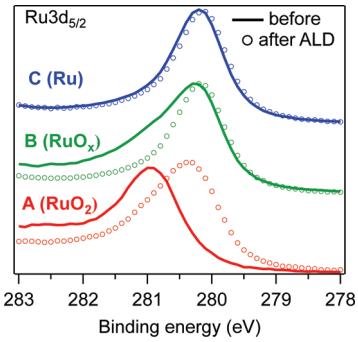

Figure 5. $Ru3d_{5/2}$ spectra of samples A–C before (lines) and after (circles) ALD of Al_2O_3. The photoemission intensities were normalized to the same maximum to enhance the changes of line-shape. For sample A were performed 15 cycles, while for sample B and C 10 and 20 cycles, respectively.

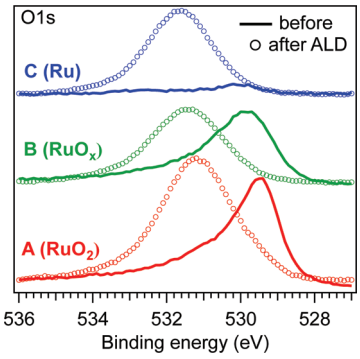

Figure 6. O1s spectra of samples A–C before (lines) and after (circles) ALD of Al_2O_3. The photoemission intensities were normalized to enhance the changes of line-shape. For sample A were performed 15 cycles, while for sample B and C 10 and 20 cycles, respectively.

included. These results are largely expected because of the different temperatures used during oxidation and agree very well with the findings of Blume et al.[39] The Ru sample has only some adsorbed oxygen due to residual gases. The amount is at the detection limit of XPS. After the deposition of about a 1 nm Al_2O_3 layer on all samples, the Ru3d spectra showed the partial reduction of RuO_2 into Ru in samples A and B (Figure 5).

The reduction of the substrate is more extensive for the sample with more O, but also the final amount of O in the substrate depends on the initial values, showing that TMA is not capable of reducing RuO_2 completely but that some Ru–O bond is still present. As will be shown below, the reduction is stopped as the first ALD layer is completed, and it does not involve the underlying RuO_2 substrate. This shows that the reduction of RuO_2 is due to the reaction of TMA directly with oxygen on the Ru–O surface and that it is not due to the diffusion of oxygen from the substrate into the thin film, as this would result in a larger amount of oxygen at the interface and a smaller one in the underlying layers. The reduction of the substrate surface can be considered equivalent to a self-limiting process, similar to the self-limiting property of ALD in depositing a fixed amount of a film in each cycle. The O1s spectra also change in shape and intensity after the deposition of Al_2O_3 (Figure 6).

Core Level Fits. In Figures 7 and 8 are reported the curve fits for the $Ru3d_{5/2}$ component and the O1s spectra before and after ALD, respectively. For all spectra, a Shirley background was first removed. The Ru3d spectra were then fitted using asymmetrical Doniach-Sunjic curves (typical for metallic samples) with the asymmetry parameter α set at 0.1. Together with the fitting curves are reported the residual curves in a different scale (5% of the spectrum scale).

The spectrum of substrate A before ALD has only the RuO_2 component at 280.8 eV (Ru^{4+}) and the satellite centered at 282.5 eV (Figure 7a). Substrate B shows an attenuated component at 280.7 eV due to either RuO_2 or RuO_x, a much stronger Ru^{0+} component centered at 280.1 eV and a weak satellite structure at lower binding energy (281.8 eV) with respect to that observed on substrate A (Figure 7b). It should be noted that because of the low resolution of the spectra (measured with a nonmonochromatic laboratory X-ray source) the distinction between the surface and subsurface RuO_x and the RuO_2 components is not possible on the basis of the Ru3d fits only. The presence of a satellite structure at low binding energy could be due to RuO_6 clusters with almost no lateral extension. However, as shown in Figure 8b, the O1s spectrum indeed confirms the presence of mostly surface and subsurface Ru–O bonds and only a small RuO_2 component. Substrate C shows an almost completely Ru^{0+} character with only a small component at about 281.6 eV due to adsorbed species (Figure 7c).

The growth of Al_2O_3 by ALD induces a change in the substrates, either by removing adsorbed and subsurface oxygen species (i.e., on the RuO_x sample, Figure 7e) or by reducing the initial Ru^{4+} to elemental Ru^{0+} (on the RuO_2 sample, Figure 7d). In the latter case, there are changes in the crystalline structure, as indicated by the strong attenuation of the RuO_2 satellite in the spectrum after ALD. That spectral feature is related to the distorted RuO_6 octahedron of the RuO_2 rutile structure:[41] its absence implies the evolution of the extended RuO_6 structure into a disordered one.[39,40] However, the Ru–O species present in sample B are embedded into the metallic Ru that has a hexagonal structure, and the RuO_6 octahedrons have a reduced lateral extension. In this case, the removal of oxygen induces smaller structural changes. Finally, sample C shows no appreciable change upon Al_2O_3 growth (Figure 7f).

The peak fit of the O1s spectra before and after ALD for samples A, B, and C (Figure 8) are made using Voigt functions[42] (mixed Gaussian–Lorentzian function) with a fixed Lorentzian width of 0.1 eV. One may note the presence of various O-species on sample A, as observed by Blume et al.[39] (Figure 8a). A considerable presence of adsorbed carbonaceous species is also found (indicated as CO_{ads} in Figure 8a–c), due to the strong reactivity of Ru surfaces toward the rest gas (oxidation was done in the ALD reactor held at a base pressure of 2×10^{-8} mbar). As noted above, substrate A has a strong component at 529.4 eV due to RuO_2 but also an intense peak at 530.1 eV due to surface and subsurface ($O_{ads,sub}$) oxygen species, and a small component at lower binding energy (528.7 eV) due to the bridge oxygen (O_{br}) on the RuO_2 surface. The small intensity here is due to the low resolution of the X-ray source used and to the scarce surface sensitivity of the Mg–Kα source. However, the small component, necessary for a good fit of the O1s peak, is a confirmation of the extended nature of RuO_2 on sample A (Figure 8a).

Substrate B also shows a small component at 529.5 eV due to some RuO_2 cluster, while the most intense component is found at 530 eV and is due to adsorbed and subsurface oxygen ($O_{ads,sub}$). As noted before, the fit of the O1s clarifies the nature of substrate B, it being impossible to discern between the bulk-like

dx.doi.org/10.1021/cm200276z |Chem. Mater. 2011, 23, 3159–3168

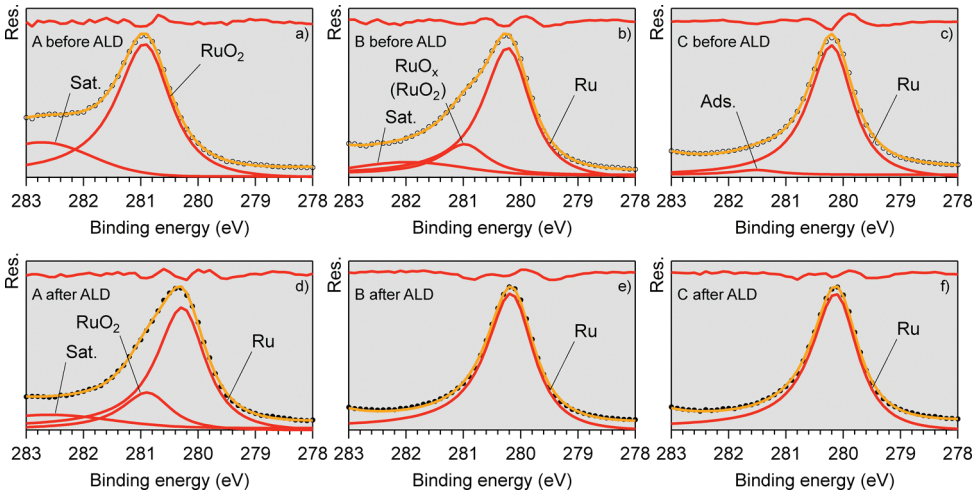

Figure 7. Peak fits of $Ru3d_{5/2}$ spectra before and after ALD. All spectra were normalized to the same height. The scale for the fit residuals is 5% of the spectrum scale.

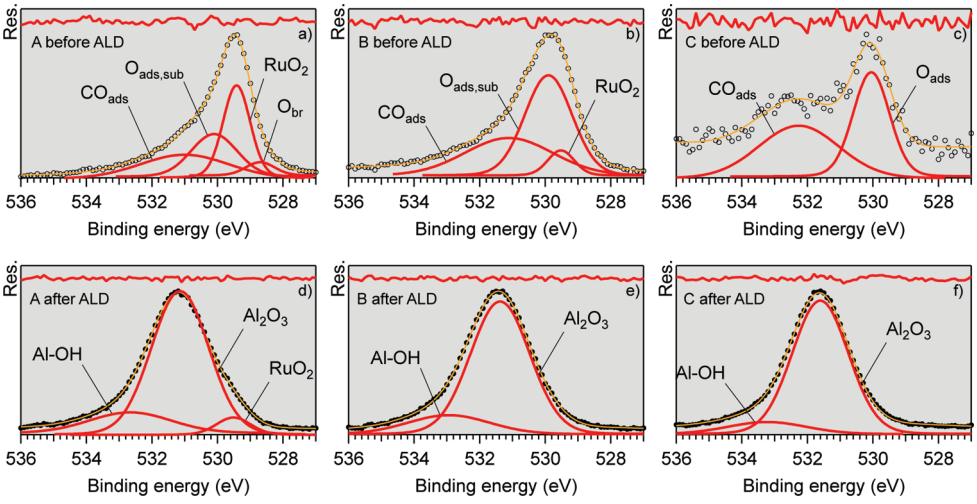

Figure 8. Peak fits of O1s spectra before and after ALD. All spectra were normalized to the same height. The scale for the fit residuals is 5% of the spectrum scale for all samples except sample C before ALD because of the very low signal/noise ratio of the measured spectra.

RuO_2 and RuO_x by looking at the Ru3d peaks, only (Figure 8b). Substrate C has a much lower O1s intensity compared to substrates A and B as it is clear by the high noise level of the spectrum. It has only some adsorbed species due to the high reactivity of the Ru surface to rest gases (Figure 8c).

Contrary to the O1s spectra before ALD, all three substrates show very similar spectra after the growth of Al_2O_3. However, some small differences may be evidenced by the curve fits. Substrate A, in fact, has three components due to Al_2O_3 (at 531.1 eV), to Al−OH (at 532.7 eV),[43] and to residual RuO_2 (at 529.5 eV) (Figure 8d). The latter is not present on substates B and C, while both have the other two components due to the Al_2O_3 layer (Figure 8e,f). As the Al−OH groups are created during the H_2O pulse and it is not surprising to find them, on the contrary, it shows that the water pulse creates the −OH termination in a similar manner in all samples. This is an important observation as it demonstrates that the initial reduction of the substrate (in A and B) does not hinder the "normal" ALD of Al_2O_3 either because the oxygen from the substrate does not react with all three CH_3 groups bonded to Al or because of the hydroxylation of the Al_2O_3 surface during the water pulse. As will be discussed below, the relative intensity between the Al_2O_3 and the Al−OH components is different between substrates A, B, and C, being (area ratio) 0.14, 0.14, and 0.09, respectively. This difference indicates that sample C has less −OH terminations on its Al_2O_3 surface, suggesting a lower density of the oxide.

Another important observation can be made regarding the binding energy of the Al_2O_3 components in the three samples. These are 531.1 eV for substrate A, 531.4 eV for substrate B, and 531.6 eV for substrate C. This difference will be discussed in the section dedicated to the electronic properties of Al_2O_3.

SR-PES before and after ALD. The synchrotron radiation spectra of the valence band (VB) and Al2p collected at 121 eV on the RuO_2 and Ru samples before and after ALD are shown in Figure 9a and b, respectively.

The initial VB spectra of the two samples are different because RuO_2 has a strong contribution of Ru4d localized very close to the Fermi level (0.6 eV), whereas Ru has a smoother behavior

dx.doi.org/10.1021/cm200276z |*Chem. Mater.* 2011, 23, 3159–3168

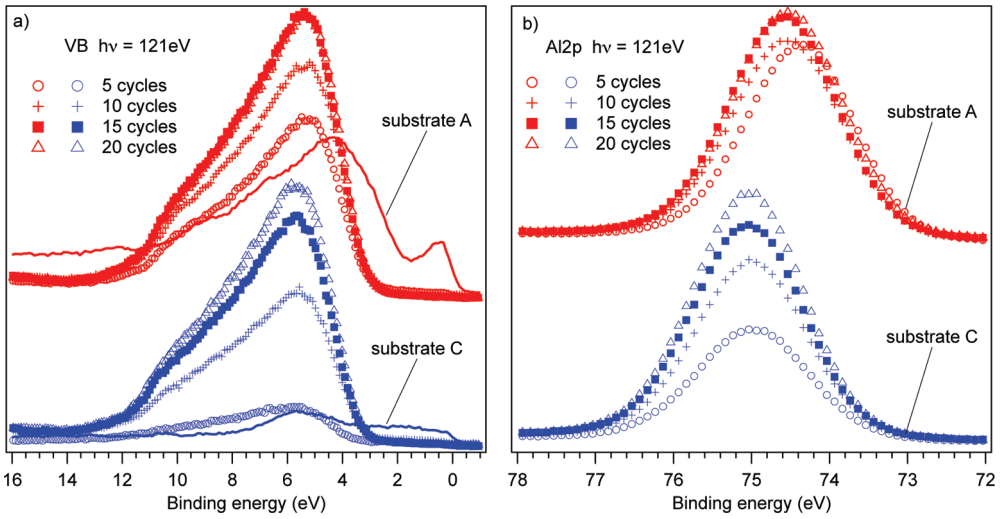

Figure 9. Valence band (a) and Al2p (b) spectra of samples A (red) and C (blue) measured with synchrotron radiation at 121 eV. All intensities were normalized to the same incoming photon flux.

near the Fermi level. Oxygen in RuO_2 is revealed by the intense peak with the maximum at about 4 eV and extending to 11 eV due to Ru4d-O2p states. ALD induces many changes, and the growth of Al_2O_3 can be followed. After the first 5 ALD cycles, the VB of the RuO_2 sample (sample A) changes markedly with a strong attenuation of the Ru4d states near the Fermi level and the transformation of the Ru4d-O2p states into Al3s3p-O2p. The VB of the Ru sample (sample C) after 5 ALD cycles also shows the growth of Al_2O_3 but at a lower rate than on RuO_2. Further ALD cycles make the behavior of the samples similar. The Al2p peaks start to increase after the first 5 cycles, and like that observed in the VB spectra, the amount of Al deposited on the RuO_2 sample after the first 5 ALD cycles is larger than that on Ru (Figure 9b).

Growth Rate Per Cycle. In order to determine the thickness of the Al_2O_3 film, one could use either the increase of the Al2p intensity or the attenuation of the Ru3d signal. However, both methods have drawbacks that would limit their application. The thickness (d) calculation by the Al2p increase is obtained using the saturation equation $I = I_0 \times (1 - exp(-d/\lambda))$. The limitation here is the empirical nature of I_0 (the saturation intensity), as it depends on the film atomic density n_{Al} (and therefore on the atomic structure and density of the film) and on the experimental conditions (photon energy, analyzer transmission function, etc.). The thickness determination by considering the substrate core level attenuation has the advantage of comparing only the initial peak area with that after film deposition ($d = -\lambda \times \ln I/I_0$, where I_0 is the intensity before deposition). However, in the present case the attenuation cannot be properly used because RuO_2 has an atomic density different from that of metallic Ru, and with I_0 being dependent on n_{Ru}, any change would induce a certain error in the thickness calculation. In our case, the attenuation of the Ru3d intensity could be used only for the Ru sample (sample C), where Ru does not change structure after the deposition of Al_2O_3. In this way, the thickness obtained by the XPS measurements after 20 ALD cycles on sample C was 1.4 nm (±0.1 nm).

Knowing the Al_2O_3 thickness on sample C, we determined the saturation intensity of the Al2p peak measured with 121 eV photons. The free electron length λ for electrons with about 50 eV kinetic energy (the Al2p electrons when excited with 121 eV photons, for example) is about 0.5 nm. This means that only

Table 2. Thickness of the Al_2O_3 Films on Samples A and C after 5, 10, 15, and 20 Cycles[a]

sample	5 ALD	10 ALD	15 ALD	20 ALD
thickness of A (nm)	1	1.1	1.4	1.7
thickness of B (nm)	0.6	0.8		
thickness of C (nm)	0.3	0.7	1.1	1.4

[a] Sample B was investigated only after 5 and 10 ALD cycles. For the description of samples A, B, and C, see Table 1.

electrons escaping from a region $3 \times \lambda = 1.5$ nm can be detected, i.e., the Al_2O_3 thickness after 20 cycles is about the saturation escape length. Therefore, we used the Al2p intensity after 20 cycles as the saturation intensity I_0 and obtained the thicknesses after each of the 5 cycles by using the Al2p intensity. We remark that this strategy is valid only for sample C (Ru). However, for samples with initial Ru−O we compared the final Al2p intensities of those samples with that of the Ru sample and consequently obtained the thickness of Al_2O_3 after each of the 5 cycles also there. The thicknesses obtained are reported in Table 2 and in Figure 10a. From those values, it is clear that the three samples behave in different ways: the Ru sample has a constant growth rate per cycle (GPC) of about 0.07 nm/cycle, whereas the RuO_2 and RuO_x samples have a large GPC during the first 5 cycles that is finally converted to the same GPC as that on the Ru sample (Figure 10a).

Hence, samples with initial Ru−O surfaces have two different growth regimes. The first regime is connected to the presence of oxygen in the substrate, as the deviation from the constant GPC is larger for sample A (with the rutile RuO_2 substrate) than for sample B (with only adsorbed and subsurface oxygen). On RuO_2, the growth takes place through the reaction of TMA with RuO_2 which reduces during the reaction, whereas on Ru, TMA reacts with −OH groups produced by H_2O in the usual ALD scheme. Won et al.[32] studied the ALD of TiO_2 on Ru from Ti tetraisopropoxide (TTIP) and observed a large GPC, addressed to the presence of oxygen in the Ru bulk that diffused toward the surface during ALD. The authors have also observed that the GPC decreased strongly when the substrate was covered by a

dx.doi.org/10.1021/cm200276z |*Chem. Mater.* 2011, 23, 3159–3168

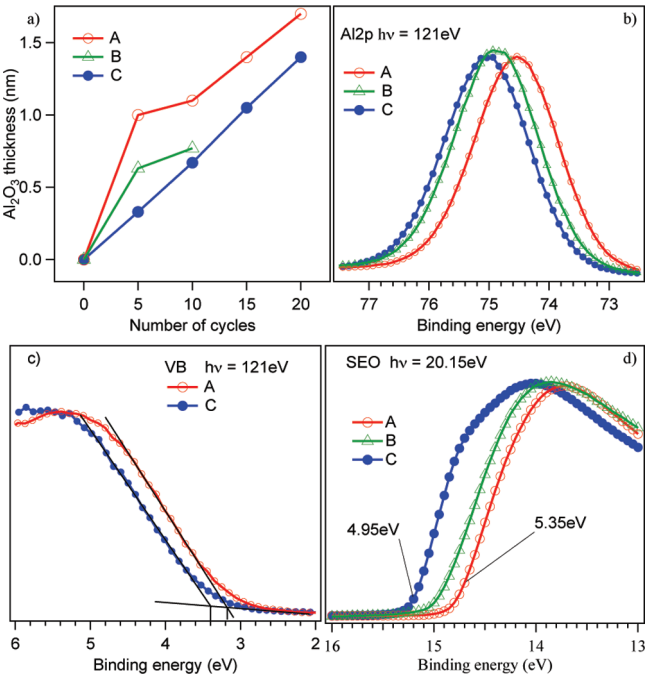

Figure 10. (a) Thickness of Al_2O_3, (b) binding energy of Al2p, (c) valence band, and (d) secondary electron offset of samples A−C. For the sake of clarity, the valence band of sample B was omitted in panel c. (b−d) Samples A and C are measured after 20 cycles, while sample B after 10 cycles.

very thin Al_2O_3 layer. They attributed that reduction to the decreased oxygen diffusion through the thin Al_2O_3 layer.

Electronic Properties of the Al_2O_3 Films. As can be observed in Figure 10b, the final binding energies (BE) of Al2p and the valence band of samples A (RuO_2) and C (Ru) depend on the initial chemical states of the substrates. However, in Figure 9b one can also observe that while the BE of Al2p does not change with increasing Al_2O_3 thickness on the Ru sample (75 eV), the Al2p on the RuO_2 sample has a low BE (74.3 eV) after 5 cycles, increases after 10 cycles (74.5 eV), and remains constant for further deposition cycles. This behavior suggests that the position of the Al2p is influenced by the presence of oxygen in the substrate, bringing a binding energy shift of 0.5 eV for films thicker than 1 nm, while thinner films have a shift of 0.7 eV.

In order to determine whether the different binding energies of the Al2p peaks on samples A and C are due to different band alignment between Al_2O_3 and the two substrates, we compare in Figure 10c the maximum of the Al_2O_3 valence band in the two samples. We find that the valence band offset (VBO) between Al_2O_3 and the Ru substrate is smaller (3.2 eV) for sample A and larger (3.45 eV) for sample C; similarly, the work function (WF) of the three samples is different, being 5.35 eV for sample A (starting RuO_2 substrate), 4.95 eV for sample C (starting Ru substrate) (Figure 10d), and having intermediate values for the RuO_x sample.

The influence of substrate composition on the WF may be due to the presence of oxygen near the Ru/Al_2O_3 interface, in agreement with the findings of Li et al.,[18] where the WF of the top electrode $Ru/RuO_x/HfO_2$ structures was observed to increase when annealing was performed in an O-rich ambient environment, and the increase was attributed to the presence of Ru−O bonds at the interface.

Table 3. Binding Energy and Work Function Differences (ΔBE and ΔWF, respectively) between Sample A and Sample C

	ΔBE(Al2p-*SR*)	ΔBE(Al2p-*MgK*α)	ΔBE(O1s)	ΔBE(VBM)	ΔWF
A−C	0.5 eV	0.5 eV	0.45 eV	0.25 eV	0.4 eV

The difference of VBO has the same sign as the Al2p shift, but it is smaller (Table 3). The change of VBO should be the same as the Al2p shift because the energy distance between a core level and the valence band maximum (VBM) is a material property. Therefore, the different behaviors of these two spectral features have to be assigned to different properties of the two Al_2O_3 films. To determine the possible reason for the different VBOs in the RuO_2 and Ru samples, the XPS measurements after the deposition of 1.4 nm Al_2O_3 on samples A and C are particularly helpful. In Figure 8d−f, we compared the O1s spectra of samples A, B, and C by peak fit.

As discussed above, the best fits were obtained by using only two components for the Ru sample, corresponding to Al_2O_3 (centered at 531.6 eV) and to Al−OH (centered at 533 eV) (Figure 8f). For the RuO_2 sample, instead, a third component at about 529.5 eV binding energy was necessary for obtaining a reliable fit (Figure 8d). This third component is due to residual Ru−O bonds under the Al_2O_3 film. We also found that the Al_2O_3 and Al−OH components of O1s in the RuO_2 sample are shifted by about 0.45 eV to lower binding energies with respect to the Ru sample, similar to the shift of the Al2p peaks and the WF difference in the two samples. Again, as shown before, sample B behaves in an intermediate way, having a smaller shift with respect to sample C. By comparing the O/Al ratio of the Al_2O_3 films on samples A and C through the intensity ratio of the O1s components and the Al2p curves, we find that the ratio is larger in the RuO_2 sample compared to that in the Ru sample. It should be noted that for the intensity of the O1s peaks, only the Al_2O_3 and Al−OH components were used, excluding the influence of the RuO_2 component in sample A on the O/Al ratio.

This indicates that the Al_2O_3 grown on the RuO_2 sample is oxygen-rich compared to that grown on the Ru sample and suggests that the different stoichiometry of the two Al_2O_3 layers could be the reason for the difference between the core level peaks and the VBM. The valence band of Al_2O_3 is due to O2p states in the upper part (lower binding energy) and to hybridized Al3s3p/O2p states in the lower part (higher binding energy). A different O/Al ratio will influence the valence band of the oxygen poor Al_2O_3, adding high binding energy states related to defects and removing lower binding energy states related to oxygen. This fact can be seen also in the valence bandwidth (VBW) of the two layers, as sample C has a larger VBW than sample A.

Furthermore, it was noted that sample A has a larger amount of Al−OH groups than sample C (Figure 8d,f), suggesting a higher density of the ALD films grown on sample A compared to that on sample C. The different chemical properties of the two samples probably derive from the different chemistries during the initial ALD cycles. The ALD on the RuO_2 sample takes advantage of the oxygen present in the substrate in two ways: (i) the steric hindrance is reduced as TMA undergoes fast reactions before the H_2O pulse, the GPC of ALD is larger, and Al_2O_3 might have a higher density; and (ii) oxygen vacancies are reduced as TMA reacts with two oxygen sources, one from RuO_2 and the other one from H_2O. However, as pointed out above, the presence

dx.doi.org/10.1021/cm200276z |*Chem. Mater.* 2011, 23, 3159–3168

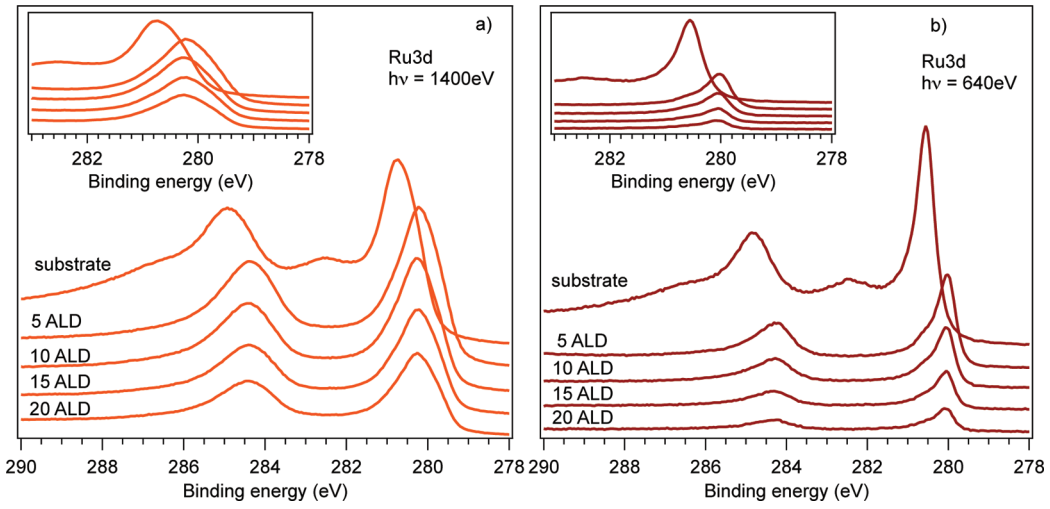

Figure 11. Ru3d spectra of sample D measured with synchrotron radiation at 1400 eV (a) and 640 eV (b). In the inset is reported the 5/2 spin−orbit component, only.

of −OH groups on top of the Al_2O_3 surface is a confirmation that the fast reactions of TMA with the oxygen from the substrate do not hinder the successive hydroxylation by the water pulse.

Detailed SR-PES after ALD. Changing the photon energy over a wide range can deliver further information about the detailed chemistry of the interface because the information depth of photoemission varies with the kinetic energy of the electrons photoemitted from a core level. To address this concern, the use of synchrotron radiation is particularly helpful and necessary. SR-PES was used here to study the changes appearing on the RuO_2^* sample after ALD of Al_2O_3. For this purpose, sample D, comparable with sample A, was used (see Table 1). The photon energies used were 350 eV, 640 eV, and 1400 eV. Considering that the kinetic energy of the Ru3d electrons (binding energy about 280 eV) is 70 eV, 360 eV, and 1120 eV, respectively, and taking into account that the emission angle was fixed to 45°, the mean free path of Ru3d electrons emitted with these photon energies is about 0.5 nm, 1 nm, and 2 nm. Two series of Ru3d spectra, measured with 640 eV and 1400 eV, are shown in Figure 11. Each series is composed of one spectrum measured on the bare substrate and four spectra after ALD. Each Al_2O_3 spectrum was measured after 5 cycles, reaching 20 cycles in total.

The initial structure of the substrate is due to RuO_2 extending in both the surface and bulk regions.[39] This is evident by the marked presence of the RuO_2 satellite at 282.5 eV and by the position of the $Ru3d_{5/2}$ spin−orbit component.[39] The latter is found at 280.7 eV in the spectrum measured with 1400 eV photons (Figure 12a) and at 280.45 eV when measured with 350 eV and 640 eV. Those binding energies correspond to the bulk RuO_2 position of $Ru3d_{5/2}$ and the position of 1f-cus-Ru, respectively.[39] The different binding energies of the $Ru3d_{5/2}$ component for different photon energies are, therefore, compatible with the formation of a bulk RuO_2 phase with 1f-cus-Ru on the surface.[39] After the deposition of Al_2O_3, the underlying substrate still has some Ru−O bonds, as shown by the peak centered at 280.3 eV in the spectra collected at 1400 eV (Figure 12b), while metallic Ru (Ru^{0+}), centered at 280 eV, is the strongest peak in the spectra measured with 640 eV and 350 eV, showing that metallic Ru is more abundant near the interface (Figure 12b). In the spectra measured with lower photon energies, a second component at about 280.5 eV is also present. This can be attributed to Ru bonded to subsurface oxygen.[39]

On the basis of these results, we may affirm that ALD leads to a depletion of oxygen near the interface, showing that, at the temperature used here, the interaction between O from the substrate and TMA is not due to the diffusion of oxygen toward the interface, in contrast to the recent investigations of Won et al.[32] This is further evidenced by the evolution of the Ru3d line shape. After the first 5 cycles, the Ru3d spectra at all photon energies change abruptly because of the RuO_2 reduction at the surface. After successive ALD cycles, instead, they do not change, showing that the chemical composition of the substrate does not change anymore (Figure 12c). If the initial reduction was also due to the diffusion of "bulk" oxygen from RuO_2, the spectrum measured with 1400 eV (more bulk sensitive) should show larger changes compared to the spectra measured with 350 eV and 640 eV (more surface sensitive). Moreover, the diffusion of oxygen from RuO_2 should continue after the formation of the first Al_2O_3 layer, and the change of the Ru3d line shape should be still present after the following ALD cycles.

Our findings could be more likely understood with an adsorption reaction, similar to the oxidative reactions in RuO_2-(110) catalysts to form only the first Al_2O_3 layer: TMA adsorbs either with a methyl group or with Al on an active site. The active sites on RuO_2 are thought to be the coordinatively unsaturated sites: the bridge O, the 1f-cus-Ru, or defects. After the adsorption of a TMA molecule, neighboring oxygen or Ru species induce the breaking of an Al-CH_3 bond leading to an Al−O bond.[40] Because of the high reactivity of CH_3 species, they could either adsorb on the surface or react to form C_2H_6 (ethane). Alternatively, the methyl group could undergo combustion reactions with oxygen producing CO, CO_2, and H_2O, as observed in O_2-based ALD of noble metals.[44]

Once the reactions take place, the Al−O complex does not desorb because of the strong bond and the low substrate temperature. Using the typical catalysis terminology, we could define the formation of Al_2O_3 on RuO_2 as a "self-poisoning" of the substrate. As the surface becomes completely covered by Al_2O_3 (poisoned catalyst), the catalytic properties of the substrate are quenched because the active adsorption sites are covered by Al_2O_3, and the growth of further Al_2O_3 is slowed.

dx.doi.org/10.1021/cm200276z |*Chem. Mater.* 2011, 23, 3159–3168

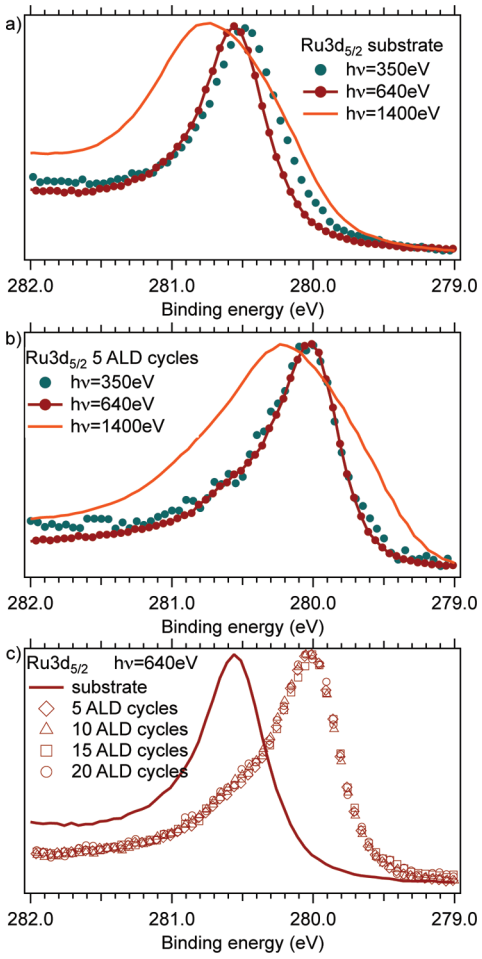

Figure 12. $Ru3d_{5/2}$ spectra of sample D measured with various photon energies. (a) The substrate before ALD and (b) after 5 ALD cycles. (c) Spectra of sample D measured with 640 eV before and after ALD. The intensities were normalized to the same peak height in order to enhance the change of line-shape.

The observation that the TMA-O reaction stops because of a lack of oxygen diffusion can explain the self-limited nature of ALD even on RuO_2 substrates with exceptionally high initial growth rate per cycle. Although the reaction of TMA with oxygen from RuO_2 is believed to take place in the first half cycle, partly removing the methyl groups from TMA during the first half cycle, the reaction could be effective only between neighboring species and could be limited to the first layer, only. The successive H_2O pulse completes the formation of Al_2O_3 and forms −OH surface groups. The second layer, hence, grows following the usual ALD procedure with ligand-exchange reactions between surface −OH groups and TMA.

This is further confirmed by observing the same GPC in both samples A and C after the first layer on sample A is completed. However, between the two GPC values, sample A goes through an intermediate step with a very slow growth rate, probably because the surface hydroxylation is not yet efficient, while the catalysis effect of RuO_2 is already quenched (Figure 10a). A possible understanding of this behavior could be the following: after the first cycle, the surface of samples A and D is probably not yet completely covered with Al_2O_3, but there could be a coexistence of Al−OH terminated regions with RuO_2 terminated ones. In this case, the growth in the next cycle still continues on RuO_2 as it is energetically favorable (because of the presence of O) and only after the complete termination of the surface with Al−OH can the "normal" ALD start.

It is also worth mentioning that in a previous investigation of the HfO_2 ALD on SiO_x by Tallarida et al., it was noted that the growth of HfO_2 starts only when a complete SiO_2 layer is formed.[45] In that case, SiO_2 forms just after 4 cycles. During the first 3 cycles, only the growth of Si suboxides was observed with almost no growth of HfO_2. The interpretation of that investigation was that only SiO_2 is effectively OH terminated and that ALD is hindered until the layer of SiO_2 is not complete.[45] Here, there could be a similar behavior, with the difference that the substrate is reduced until a complete layer of Al_2O_3 is formed; after this, an OH termination is also needed to start the "normal" ALD.

CONCLUSIONS

The ALD of Al_2O_3 on Ru and RuO_2 has been studied by means of photoelectron spectroscopy using both anode X-ray source and synchrotron radiation. We found that the growth of Al_2O_3 depends on the degree of oxidation of the substrate. The growth rate per cycle was initially enhanced by the presence of oxygen in the substrate, but it turned out to the same value as that observed for the ALD on pure Ru after the formation of one Al_2O_3 layer. We conclude that the GPC enhancement occurs only in the first cycles because of a direct TMA-O reaction during the TMA pulse. After the full coverage of the surface, however, oxygen from the substrate does not participate anymore in ALD, and the GPC is due to hydrolysis as in the "normal" ALD with ligand-exchange reactions. This last finding shows that the enhanced ALD growth is due to the active participation of oxygen from the substrate in the ALD reactions and that it is not connected with the diffusion of oxygen from the RuO_2 film.

It is worth noting that our results are partially different from those recently published by Lee et al.,[33] where the authors observed the RuO_2 reduction upon reaction with titanium diisopropoxide bis(tetramethylheptadionate) ($Ti(O\text{-}iPr)_2(tmhd)_2$). Although Lee et al. observed an increased GPC on RuO_2 with respect to Ru, they also showed that, depending on the oxygen source, a constant growth rate per cycle occurred when water was used as the oxygen source, while a surface enhanced growth was present when they used O_3. In this latter case, the authors observed the reoxidation of Ru during the O_3 pulse. On the contrary, we had the surface enhanced growth even using water as the oxygen source, although the reoxidation of Ru was not present.

The use of synchrotron radiation allowed us to establish that different substrates did induce not only different growth behaviors of Al_2O_3 but also different physical properties of the entire system. ALD performed on samples with different substrate composition showed different binding energies of the Al_2O_3 related peaks and a change of WF. The different binding energies of core level peaks and valence band maxima revealed the different band alignments between Al_2O_3 and the substrates, depending on their initial oxygen content. A similar dependence was found for the WF.

The different WFs agree with previous studies on HfO_2/Ru structures, where the oxidation of a top Ru electrode, performed by post-deposition annealing in O_2,[18] induced an increase of the WF, attributed to an oxygen enrichment at the Ru/HfO_2

dx.doi.org/10.1021/cm200276z |*Chem. Mater.* 2011, 23, 3159–3168

interface. Here, although the WF had larger values on the substrates with larger initial oxygen content, as shown by Li et al.,[18] we find that the interface is oxygen depleted in a similar way in all samples studied, independently from the initial conditions. Finally, the VBO between the substrate and Al_2O_3 was dependent on the substrate treatment before ALD depending on both the WF of the substrate and the O/Al ratio. The latter was found to be higher for the oxide grown on RuO_2 as a result of the oxygen-assisted ALD during the first cycles. In conclusion, we showed that the chemical and physical properties of the Al_2O_3/Ru system are strongly dependent on substrate pretreatment because of the occurrence of different chemical reactions.

AUTHOR INFORMATION

Corresponding Author

*Phone: +49 (0)355 693099. Fax: +49 (0)355 693139. E-mail: tallamas@tu-cottbus.de.

ACKNOWLEDGMENT

We thank R. Blume (FHI-Berlin) for precious suggestions. Partially, the study has been supported by the German Ministry of Education and Research, the Academy of Finland, and the Estonian Ministry of Education and Research.

REFERENCES

(1) Suntola, T. *Thin Solid Films* **1992**, *216*, 84.
(2) Masel, R. I. *Principles of Adsorption and Reaction on Solid Surfaces*; Wiley: New York, 1996.
(3) Kim, S. K.; Hwang, G. W.; Kim, W.-D.; Hwang, C. S. *Electrochem. Solid-State Lett.* **2006**, *9*, F5.
(4) Choi, G.-J.; Kim, S. K.; Lee, S. Y.; Park, W. Y.; Seo, M.; Choi, B. J.; Hwang, C. S. *J. Electrochem. Soc.* **2009**, *156*, G71–G77.
(5) Lüth, H. *Solid Surfaces, Interfaces and Thin Films*, 4th ed.; Springer: Berlin, Germany, 2001.
(6) Baker, L.; Cavanagh, A. S.; Seghete, D.; George, S. M.; Mackus, A. J. M.; Kessels, W. M. M.; Liu, Z. Y.; Wagner, F. T. *J. Appl. Phys.* **2011**, *109*, 084333.
(7) Kukli, K.; Aarik, J.; Aidla, A.; Uustare, T.; Jõgi, I.; Lu, J.; Tallarida, M.; Kemell, M.; Kiisler, A.-A.; Ritala, M.; Leskelä, M. *J. Cryst. Growth* **2010**, *312*, 2025.
(8) Mars, P.; van Krevelen, D. W. *Chem. Eng. Sci. Spec.* **1954**, Suppl. 3, 41.
(9) Doornkamp, C.; Ponec, V. *J. Mol. Catal. A: Chem.* **2000**, *162*, 19.
(10) Widjaja, Y.; Musgrave, C. B. *Appl. Phys. Lett.* **2002**, *80*, 3304.
(11) Halls, M. D.; Raghavachari, K. *J. Chem. Phys.* **2003**, *118*, 10221.
(12) Jeloaica, L.; Estève, A.; Djafari Rouhani, M.; Estève, D. *Appl. Phys. Lett.* **2003**, *83*, 21.
(13) Elliott, S. D.; Pinto, H. P. *J. Electroceram.* **2004**, *13*, 117.
(14) Shi, Y.; Sun, Q.-Q.; Dong, L.; Liu, H.; Ding, S.-J.; Zhang, W. *Chin. Phys. Lett.* **2009**, *26*, 053101.
(15) Zhao, C.; Pawlak, M. A.; Popovici, M.; Schaekers, M.; Sleeckx, E.; Vancoille, E.; Wouters, D. J.; Tokei, Zs.; Kittl, J. A. *ECS Trans.* **2009**, *25* (4), 377.
(16) Zhong, H.; Heuss, G.; Misra, V.; Luan, H.; Lee, C.-H.; Kwong, D.-L. *Appl. Phys. Lett.* **2001**, *78*, 1134.
(17) Rangan, S.; Bersch, E.; Bartynski, R. A.; Garfunkel, E.; Vescovo, E. *Phys. Rev. B* **2009**, *79*, 075106.
(18) Li, Z.; Houssa, M.; Schram, T.; De Gendt, S.; De Meryer, K. *Appl. Phys. Lett.* **2009**, *95*, 183506.
(19) Burke, L. D.; Naser, N. S.; Sharna, R. *J. Appl. Electrochem.* **2008**, *38*, 377.
(20) Kim, S. K.; Hoffmann-Eifert, S.; Waser, R. *ECS Trans.* **2009**, *25* (4), 289.
(21) Kim, W.-H.; Park, S.-J.; Kim, D. Y.; Kim, H. *J. Korean Phys. Soc.* **2009**, *55*, 32.
(22) Park, S.; Kanjolia, R.; Anthis, J.; Odedra, R.; Boag, N.; Wielunski, L.; Chabal, Y. *Chem. Mater.* **2010**, *22*, 4867.
(23) Li, Q.; Li, K. B.; Huan, A. C. H.; Chai, J. W.; Pan, J. S.; Ong, C. K. *Appl. Phys. Lett.* **2004**, *85*, 6155.
(24) Over, H.; Kim, Y. D.; Seitsonen, A. P.; Wendt, S.; Lundgren, E.; Schmid, M.; Varga, P.; Morgante, A.; Ertl, G. *Science* **2000**, *287*, 1474.
(25) Böttcher, A.; Starke, U.; Conrad, H.; Blume, R.; Gregoratti, L.; Kaulich, B.; Barinov, A.; Kiskinova, M. *J. Chem. Phys.* **2002**, *117*, 8104.
(26) Over, H.; Knapp, M.; Lundgren, E.; Seitsonen, A. P.; Schmid, M.; Varga, P. *Chem. Phys. Chem.* **2004**, *5*, 167.
(27) Halls, M.; Raghavachari, K.; Frank, M. M.; Chabal, Y. *Phys. Rev. B* **2003**, *68*, 161302.
(28) Goldstein, D. N.; McCormick, J. A.; George, S. M. *J. Phys. Chem. C* **2008**, *112*, 19530.
(29) Juppo, M.; Rahtu, A.; Ritala, M.; Leskelä, M. *Langmuir* **2000**, *16*, 4034.
(30) Wind, R. W.; Fabreguette, F. H.; Sechrist, Z. A.; George, S. M. *J. Appl. Phys.* **2009**, *105*, 074309.
(31) Puurunen, R. *J. Appl. Phys.* **2005**, *97*, 121301.
(32) Won, S.-J.; Suh, S.; Lee, S. W.; Choi, G.-J.; Hwang, C. S.; Kim, H. J. *Electrochem. Solid-State Lett.* **2010**, *13*, G13.
(33) Lee, S. W.; Han, J. W.; Kim, S. K.; Han, S.; Lee, W.; Hwang, C. S. *Chem. Mater.* **2011**, *23*, 976.
(34) Tallarida, M.; Karavaev, K.; Schmeisser, D. *J. Appl. Phys.* **2008**, *104*, 064116.
(35) Tallarida, M.; Weisheit, M.; Kolanek, K.; Michling, M.; Engelmann, H.-J.; Schmeisser, D. *J. Nanopart. Res.* **2011**10.1007/s11051-011-0319-x.
(36) Kukli, K.; Kemell, M.; Puukilainen, E.; Aarik, J.; Aidla, A.; Sajavaara, T.; Laitinen, M.; Tallarida, M.; Sundqvist, J.; Ritala, M.; Leskelä, M. *J. Electrochem. Soc.* **2011**, *158*, D158.
(37) Schmeisser, D.; Hoffmann, P.; Beuckert, G. *Materials for Information Technology, Devices, Interconnects and Packaging, Engineering Materials and Processes*; Springer: New York, 2005.
(38) Madhavaram, H.; Idriss, H.; Wendt, S.; Kim, Y. D.; Knapp, M.; Over, H.; Assmann, J.; Löffler, E.; Muhler, M. *J. Catal.* **2001**, *202*, 296.
(39) Blume, R.; Niehus, H.; Conrad, H.; Böttcher, A.; Aballe, L.; Gregoratti, L.; Barinov, A.; Kiskinova, M. *J. Phys. Chem. B* **2005**, *109*, 14052.
(40) Knop-Gericke, A.; Kleimenov, E.; Hävecker, M.; Blume, R.; Teschner, D.; Zafeiratos, S.; Schlögl, R.; Bukhtiyarov, V. I.; Kaichev, V. V.; Prosvirin, I. P.; Nizovskii, A. I.; Bluhm, H.; Barinov, A.; Dudin, P.; Kiskinova, M. *Adv. Catal.* **2009**, *52*, 213.
(41) Over, H.; Seitsonen, A. P.; Lundgren, E.; Smedh, M.; Andersen, J. N. *Surf. Sci. Lett.* **2002**, *504*, L196.
(42) Armstrong, B. H. *J. Quant. Spectrosc. Radat. Transfer.* **1967**, *7*, 61.
(43) Aguirre-Tostado, F.; Milojevic, M.; Lee, B.; Kim, J.; Wallace, R. *Appl. Phys. Lett.* **2008**, *93*, 172907.
(44) Aaltonen, T.; Ritala, M.; Sajavaara, T.; Keinonen, J.; Leskelä, M. *Chem. Mater.* **2003**, *15*, 1924.
(45) Tallarida, M.; Karavaev, K.; Schmeisser, D. *ECS Trans.* **2009**, *25*, 253.